JPET Fast Forward. Published on May 13, 2013 as DOI: 10.1124/jpet.113.205476

TITLE PAGE

The grasshopper: A novel model for assessing vertebrate brain uptake

Olga Andersson, Steen Honoré Hansen, Karin Hellman, Line Rørbæk Olsen, Gunnar Andersson, Lassina Badolo, Niels Svenstrup, Peter Aadal Nielsen

EntomoPharm R&D, Medicon Village, S-223 81 Lund, Sweden (OA, KH, GA, PAN)

Department of Pharmacy, Faculty of Health and Medical Sciences, University of Copenhagen, DK-2100 Copenhagen, Denmark (SHH, LRO)

Division of Discovery Chemistry and Drug Metabolism and Pharmacokinetics, H. Lundbeck A/S, Ottiliavej 9, 2500 Copenhagen, Denmark (LB, NS)

JPET Fast Forward. Published on May 13, 2013 as DOI: 10.1124/jpet.113.205476
This article has not been copyedited and formatted. The final version may differ from this version.

RUNNING TITLE PAGE

Running title: A novel model for assessing vertebrate brain uptake

Corresponding should be addressed to: Peter Aadal Nielsen; pan@entomopharm.com; Phone: +46 (0) 702-175059; EntomoPharm R&D, Medicon Village, S-223 81 Lund, Sweden

Text pages: 23

Tables: 2

Figures: 5

References: 28

Abstract: 248 words

Introduction: 745 words

Discussion: 1493 words

Nonstandard abbreviations: Pgp, P-glycoprotein; BBB, blood brain barrier; CNS, central nervous system; ko, knockout; MDCK, Madin-Darby canine kidney; MDR1 multidrug resistance protein-1; MDCK-MDR1,MDR1-transfected MDCK; B/P, brain-plasma ratio; CsA, Cyclosporine A; liquid chromatography-mass spectrometry (LC-MS)

JPET Fast Forward. Published on May 13, 2013 as DOI: 10.1124/jpet.113.205476
This article has not been copyedited and formatted. The final version may differ from this version.

Abstract

The aim with the present study is to develop a blood-brain barrier (BBB) permeability model, which is applicable in the drug discovery phase. The BBB ensures proper neural function but it restricts many drugs from entering the brain and this complicates the development of new drugs against central nervous system diseases. Many in vitro models have been developed to predict BBB permeability but the permeability characteristics of the human BBB are notoriously complex and hard to predict. Consequently, one single suitable BBB permeability screening model, which is generally applicable in the early drug discovery phase, does not yet exist. A new refined ex vivo insect based BBB screening model that uses an intact, viable whole brain under controlled 'in vitro' like exposure conditions is presented. This model uses intact brains from dessert locusts, which are placed in a well containing the compound solubilized in an insect buffer. After a limited period of time the brain is removed and the compound concentration in the brain is measured by conventional LC-MS. The data presented here includes 25 known drugs and the data shows that the ex vivo insect model can be used to measure the brain uptake over the hemolymph-brain barrier of drugs and that the brain uptake shows linear correlation with in situ perfusion data obtained in vertebrates. Moreover, this study shows that the insect ex vivo model is able to identify Pgp substrates and the model allows differentiation between low permeability compounds and compounds that are Pgp substrates.

Introduction

The vertebrate blood brain barrier (BBB) is composed of capillary endothelial cells that control the entry of nutrients and xenobiotics to the brain and ensures an optimal environment for proper neural function (Abbott et al., 2006; Abbott et al., 2010). However, the BBB creates a great obstacle for the medical treatment of diseases related to the central nervous system (CNS) and it is recognized as a major obstacle in the discovery of new drugs against CNS related diseases (Geldenhuys et al. 2012). Therefore, a number of cell based in vitro models have been developed and used as tools in the drug discovery screening process (Polli et al., 2001; Weiss et al., 2003; Mensch et al., 2009). Two commonly employed systems are the renal cell lines LLC-PK1 and MDCK. Both are easy to grow and this makes them attractive for industrial use. However, these cells are of epithelial origin and compared to barrier endothelial cells, epithelial cells display differences in morphology, tight junction organization and transporter expression (Garberg et al., 2005; Cecchelli et al. 2007; Abbott et al, 2008; Liu et al. 2008). Recently, we presented an insect based BBB screening model that uses an intact whole brain under controlled 'in vitro' like exposure conditions (Nielsen et al. 2011). As in vertebrates the protection of the insect CNS requires a tight brain barrier containing influx and efflux transporter proteins which control elements entering the brain (Bundgaard and Abbott, 2008; DeSalvo et al., 2011; Stork et al. 2008; Banerjee and Bhat, 2006). Insect brain barrier consists of glia cells which are the most abundant cell type in the vertebrate CNS. Paracellular diffusion in insects is controlled by septate/tight junctions that are homologous to tight junctions controlling paracellular diffusion in vertebrates (Danemann and Barres, 2005; Freeman and Doherty, 2006; Wu and Beitel, 2004).

Transporters are present in the insects and it has been shown that the human MDR1 antibody (c219) binds to the MDR65, i.e.an insect MDR1 homologue present in the insect brain barrier (Mayer et al., 2009). Functionally we have shown that the Pgp inhibitor verapamil blocks the efflux of Pgp

substrates (Nielsen et al., 2011). This study concluded that insect models can be used as models to identify Pgp substrates. The structural and functional similarities of the vertebrate and invertebrate BBB enables the use of invertebrates as advanced screening models for BBB permeability determinations.

Previously, two different insect based BBB permeability models model have been reported (Nielsen et al., 2011). One model is a traditional in vivo model where the substance of interest is injected directly into abdomen and the brain and the body fluid (hemolymph) concentrations are measured. The brain-hemolymph ratio gives an estimate of the ability of the compound to permeate the BBB. However, as in vertebrates the insect in vivo results are influenced by a number of parameters like unspecific protein binding, metabolism, distribution, and elimination and this makes it complex to translate brain-hemolymph ratios into BBB permeability. To reduce this complexity we have developed a second model, the ex vivo model. In this model the intact brain is dissected from the insect and place in a well containing the compound of interest (Figure 1). Insects are characterized by their exoskeleton where the organs are surrounded by the hemolymph, which is circulated by the heart. No capillaries are present in insects and they are not depending on circulation of the hemolymph through the organs. This allows dissection of the brain before compound exposure and the absence of capillaries in the insect brain eliminates any contribution from residual blood in brain.

The ex vivo BBB permeability model is unique since the biologic events outside the brain are removed. Despite this the brain barrier is intact and all mechanisms and biological events inside the brain are preserved.

In this study we use the ex vivo grasshopper model to measure the brain uptake to assess the BBB permeability of 25 known drugs. The insect brain uptake is compared with in perfusion data from the literature and linear correlation between ex vivo and in situ brain uptake is found. The ex vivo

JPET Fast Forward. Published on May 13, 2013 as DOI: 10.1124/jpet.113.205476
This article has not been copyedited and formatted. The final version may differ from this version.

conditions ensure that the exposure concentration is controllable and constant during an experiment and this feature is used to investigate concentration dependent permeabilities. The ex vivo data at high exposure concentrations correlates remarkably well to vertebrate in situ data. Moreover, it is shown that ex vivo data obtained at low exposure concentrations allows identification of Pgp substrates by co-administration with the Pgp inhibitor verapamil.

JPET Fast Forward. Published on May 13, 2013 as DOI: 10.1124/jpet.113.205476
This article has not been copyedited and formatted. The final version may differ from this version.

Materials and methods

Animals. Desert locusts, *Schistocerca gregaria* (L), are obtained from a commercial animal breeder (Petra Aqua, Prague, Czech Republic). At arrival the locusts were housed under crowded conditions in an insect room and adapted to a 12:12 hours dark/light cycle. The locusts were maintained in colonies at a local terrarium temperature of 30^{o}C to 34^{o}C. The animals were fed Chinese cabbage, fresh grass, and wheat bran ad libitum. All experiments were carried out on fifth instar locusts and 2 to 3 weeks after adult emergence.

Chemicals. All drugs used in the insect ex vivo studies and HEPES were purchased from Sigma-Aldrich (Stockholm, Sweden). The drugs used in MDCK-MDR1 experiments to determine were available from Lundbeck in-house sources. All other chemicals were analytical reagent grade.

Reference Set Selection. 25 known drugs were selected from the literature with the objective to have a balanced number of known CNS and non-CNS drugs. To avoid any ambiguity the therapeutic indication of the selected compounds should be either CNS or peripheral. The selected drugs are representative for the marketed drugs in terms of LogP, molecular weight, number of H-bond donors and acceptors and the set contains neutrals, acidic and basic drugs. Moreover, the selected set contains known CNS drugs, which are known efflux substrates and passively diffusing compounds.

MDCK-MDR1 experiments. MDR1-MDCK cells originate from transfection of Madin Darby canine kidney (MDCK) cells with the MDR1 gene, the gene encoding for Pgp. MDCK-MDR1 cells (obtained from Piet Borst at the Netherlands Cancer Institute) were seeded onto polyethylene membranes in 96-well BD insert systems at 2×10^{5} cells/cm^{2} until to 4–6 days for confluent cell

monolayer formation. Test compounds (2 μM) were applied to the top (A) or bottom (B) side of the cell monolayer. Permeation of the test compounds from A to B direction or B to A direction was determined in triplicate over a150-min incubation at 37 °C and 5% CO2 with a relative humidity of 95%. In addition, the efflux ratio of each compound was also determined. Test and reference compounds were quantified by liquid chromatography- mass spectrometry (LC-MS) or LC-MS/MS analysis based on the peak area ratio of analyte/IS

Ex vivo experiments. Test solution preparation: Stock solutions were prepared by dissolving the test compounds in DMSO. Final test solution concentrations were obtained by diluting stock solutions with insect buffer (NaCl 147 mM, KCl 10 mM, $CaCl_2$ 4 mM, NaOH 3 mM and HEPES 10 mM (pH 7.2)).

Ex vivo experiment procedure (Figure 1): The brain was dissected by cutting off the frontal part of the head, through the esophagus. The three merged ganglia of the brain (protocerebrum, deutocerebrum and tritocerebrum) were prepared by using fine forceps. The brain was dissected free from fat and placed in a microwell plate (96U Microwell; Nunc) containing 250 µl of the test compound dissolved in the insect buffer. The experiments are run at 30^{o}C in a block thermostat (HLC, Germany). After a standard exposure time of 15 minutes the brains were removed from the wells, and washed twice in ice cold insect buffer. Before transfer to the test tubes the neural lamella surrounding the brain was removed. After addition of 150 µl of 2% zinc sulfate in 50% methanol the brain tissue was homogenized by means of ultrasonicaton (Bandelin *electronic*, Germany) for 8 seconds at a power of 19%. After centrifugation at 10 000 x g for 5 minutes at 4^{o}C the supernatant was analyzed by high performance liquid chromatography- mass spectrometry (LC-MS). The ex vivo studies are performed as triple tests with two brains pooled in each test tube, i.e. a total of 6 brains in each study (Figure 1).

Analysis of the quantity of drugs in insect brain tissue. The supernatant from the brain homogenates were analyzed by LC-MS using an Agilent 1200 HPLC coupled to a MSD 1100 detector (Agilent Technologies, Walbronn, Germany). The chromatographic column was a Phenomenex Kinetex C_{18} (Værløse, Denmark), 50 x 4.6 mm with 2.6 µm particles and was kept at 30°C. The mobile phase A was 0.1% formic acid and mobile phase B was 0.1% formic acid in methanol and analysis was performed using gradient elution from 5 to 90% mobile phase B. Detection was performed in SIM mode using the appropriate $[M+1]^+$ ions in positive mode.

Calculation of brain compound concentration. The concentration measured by LC-MS equals the brain concentration of two brains diluted in 150 µl 50% MeOH with 2% v/W ZnSO4 and 500nM Caffeine. The weight of an average dessert locust brain is 1.6 µg and it is assumed that this weight equals a volume of 1.6 µl. Thus, to calculate the compound brain concentration the concentration measured by LC-MS is multiplied by 150 µl and divided by 2x1.6 µl.

Statistical analysis. All values are expressed as mean ± standard deviation (S.D.). To determine statistical significantly differences among the experimental groups, the single-tailed student's t-test was used. A *p* value of less than 0.05 was termed significant.

Results

Table 1 details the compound reference set used in the present study. The set includes 13 known CNS drugs and 12 known peripheral drugs and they all cover a wide range of physico-chemical properties. The reference set includes acidic, neutral, basic and zwitterionic substances. The molecular mass varies from 194 to 1203 g/mol and the lipophilicity varies from -2.2 to 5.5.

Results from MDCK-MDR1

The apparent permeability coefficients (Papp) have been obtained by MDCK-MDR1 cells for 14 compounds using the method described above while Papp for 7 have been extracted from the literature (Di et al., 2009) (Table 1). The measured permeability coefficients range from 78 to $0.1x10^{-6}$ cm/sec. Eight of the known CNS drugs including warfarin are characterized by Papp above $10x10^{-6}$ cm/sec; Papp for four CNS drugs: risperidone, fluoxetine, amitriptyline and desipramine are in the range between 5 and 10 $x10^{-6}$ cm/sec. Compounds with Papp below $5x10^{-6}$ cm/sec are paroxetine and eight peripheral acting drugs.

Results from ex vivo brain uptake

The uptake in the insect brain was measured after 15 minutes in a 10 μM exposure concentration of the compound test solution. Compounds characterized by high concentrations in the insect brain are assumed to have high BBB permeability and they are likely to enter the vertebrate brain. The brain concentrations are displayed in Figure 2 and the data showed that all CNS active compounds in the reference set are present in the insect brain in high concentrations. Generally, the peripheral acting compounds in the reference set were present in the insect brain in low concentrations i.e. reflecting low brain uptake in vertebrates. From the data shown in Figure 2 it is seen that there is a group of compounds, which may be classified as intermediate permeating compounds. The intermediate

group includes the peripheral drugs: cetirizine, quinidine and loperamide. These three drugs are all known Pgp substrates in vertebrates. In previous studies it has been seen that high exposure concentrations in the ex vivo model may saturate transporters and this may diminishing the efflux or influx mechanism (Nielsen et al., 2011). To reduce the risk of saturation of the transporters we decided to study the brain uptake at lower exposure concentration.

In Figure 3 the measured insect brain concentrations of the reference compounds are shown when using exposure concentrations of 3 μM. As it is seen there is a separation between peripheral and CNS active drugs. All peripheral compounds are those present in lowest concentrations in the insect brain.

As expected, the measured insect brain concentrations are highly dependent on the exposure concentration and for all compounds in the reference set the measured insect brain concentration at 3 μM exposure is lower than at 10 μM. Reduction of the exposure concentration from 10 to 3 μM does not always lead to a 3-fold reduction of the brain concentration, i.e. there is not a linear relation between exposure and uptake for all compounds.

Identification of Pgp substrates

To identify the Pgp substrates in the present reference set the compounds were co-administered with the Pgp inhibitor verapamil, which blocks the efflux of Pgp substrates. In this study the brain uptake of compounds that are not Pgp substrates should not be influenced by co-administration with Verapamil while an increased brain concentration is expected for Pgp substrates. Here we use the compound exposure concentration of 3 μM and the verapamil concentration is 25 μM. To identify Pgp substrates we calculated the ratio between the measured brain concentrations when the compound is co-administered with verapamil (Ctot + verapamil) and the brain concentration measured when no verapamil has been added (Ctot), Table 2. In Table 2, Pgp substrates are defined

as compounds with a ratio above 1.5 and compounds where the brain uptake is significantly increased after co-administration with verapamil.

By applying this definition to the reference data set we get the classification of the compounds as shown in Table 2. As can be seen ten compounds are classified as Pgp substrates while eight are non-Pgp substrates. Haloperidol, fluoxetine, and amitriptyline have been removed due to large standard deviations (see Table 1), which make classification of these compounds ambiguous. The brain uptake of ranitidine, lincomycin, atenolol, and methotrexate are below detection limit (i.e. below 0.09 μM) both with and without co-administration with verapamil and data for these compounds are not included in Table 2.

As it is seen in Table 1 there is generally a low standard deviation in each experiment and no outliers have been removed in the reported data. To investigate the stability of the ex vivo insect model we repeatedly measured the barrier integrity and function. The paracellular function was measured as atenolol permeability while cabamazepine was used to test passive diffusion and the physiologic status was defined as quinidine exclusion and Pgp inhibition. During a period of ten months repeated studies of the passively diffusing compound cabamazepine and the efflux substrate quinidine showed variation ranges of 13-18% and 12-25%. The size of the desert locust brain in male is 1.60 +/- 0.09 mg while female brain is 1.68 +/- 0.16 mg (in both cases n=12) corresponding to variation of 6 and 10% respectively. Thus, brain size differences are not expected to be any significant source of error.

JPET Fast Forward. Published on May 13, 2013 as DOI: 10.1124/jpet.113.205476
This article has not been copyedited and formatted. The final version may differ from this version.

Discussion

Ex vivo brain uptake: All CNS drugs in the reference set are characterized by a high in brain uptake, i.e. none of the CNS active compounds were identified as false negatives. Moreover, it is seen that compounds in the reference set can be classified in three different groups according to the measured insect brain concentrations:

- **High** permeable, i.e. compounds with obvious CNS potential
- **Intermediate** permeable, i.e. compounds that require more investigation
- **Low** permeable, i.e. compounds without obvious CNS potential

At 10 μM the intermediate group includes both CNS drugs and Pgp substrates. Previous studies have shown that high exposure concentration of Pgp substrates may saturate the transporter, which diminish the Pgp efflux (Nielsen et al., 2011). Thus, at 10 μM Pgp substrates may start to saturate of the efflux mechanism and this potentially leads to characterization of Pgp substrates as intermediate permeable. Reduction of the exposure concentration reduces the risk for saturation and at 3 μM the Pgp substrates are removed from the intermediate group. At 3 μM all peripheral acting drugs are characterized as those displaying the lowest brain uptake.

BBB permeability: The exposure time in the insect ex vivo model is 15 minutes and the exposure concentration is considered constant during the entire experiment. In addition, the model does not contain any plasma proteins and no metabolic enzymes are present in the exposure solution. Thus, as it is the case with in vitro permeability models the ex vivo model is expected to correlate with LogPS obtained by in situ perfusion experiments, which is the gold standard for permeability measurements (Dagenais et al., 2009). To evaluate the capability of the ex vivo model to predict

BBB permeabilities we use rodent perfusion in situ data extracted from Dagnais et al. It has previously been shown that there is a close 1:1 relationship between LogPS obtained in mice and rats (Murakami et al., 2000). Thus, despite that the in situ data used in this study are generated at different laboratories and come from different species we consider them still as being useful as benchmarking data. If available we have used in situ data obtained in either MDR1 knockout (ko) mice or from experiments where Pgp has been blocked by a Pgp inhibitor (Table 1).

In vitro apparent permeability coefficients (Papp) have been obtained by using MDCK-MDR1 cells characterized by overexpression of Pgp. Thus, correlation between Papp and in situ LogPS is only expected to be seen for compounds known to be non-Pgp substrates. However, as it is seen in Figure 4a there is no correlation between the in situ data extracted from Dagenais et al. and MDCK-MDR1 data extracted from Di et al.(Di et al., 2009) or generated in this study. As it has been shown by Di et al. the MDCK-MDR1 data does not correlate with in situ perfusion data and there are a number of compounds that are detected as false positives and even more problematic false negatives, i.e. CNS drugs that are low or non-permeating in the MDCK-MDR1 assay.

The insect ex vivo brain uptake data at 10 μM shows a strong correlation (R^2=0.88) with the in situ data, Figure 4b. These data indicate that the ex vivo insect model gives a quantitative measurement of the brain uptake that corresponds to in situ data. At 10 μM exposure concentration the Pgp transporters start to be saturated. Thus, the observed remarkable good correlation between the in situ LogPS and Ctot at 10 μM is likely to be due to the fact that the Pgp efflux is diminished in both cases.

It is well-know that transporter systems may be saturated at high exposure concentrations and this will influence BBB permeability measurements (Nielsen et al. 2011, Mahar et al. 2002). To avoid saturation of the transporters in the ex vivo system the exposure concentration was reduced to 3 μM and BBB permeability plus Pgp efflux was investigated. As seen in Figure 4c the correlation

coefficient between Ctot at 3 μM and LogPS is lower than at 10 μM exposure, i.e. R^2=0.83 versus R^2=0.88 respectively. Co-exposure at 3 μM with Verapamil increases the correlation between the measured insect brain concentration and LogPS, R^2=0.85. Thus, there is slightly stronger correlation between LogPS and insect brain concentrations when the insect transporters are partly saturated (at 10 μM) or when the insect Pgp analogue is blocked by co-administration with verapamil.

In MDCK the permeability is assessed by a cell layer while the ex vivo and in situ model use brains containing brain tissues. The brain uptake measured in the insect ex vivo is influenced by the brain tissue binding (unpublished results) and the correlation to in situ data makes it reasonable to believe that brain tissue binding also has impact on the in situ perfusion data. Thus, the MDCK and the ex vivo model may complement each other where the former gives a raw permeability assessment while the latter an alternative to in situ or in vivo B/P measurements.

The brain tissue has a high content of fat and this may increase the uptake of lipophilic compounds in the brain. As it is seen in Figure 5 there is a linear dependency between lipophilicity and uptake measured by the in situ and ex vivo at 10 μM, correlation coefficients are 0.70 and 0.64 respectively. Ex vivo data obtained at 3 μM exposure hardly correlates to lipophilicity (R^2=0.46) and the correlation coefficient increases to 0.57 using 3 μM exposure plus verapamil. This suggests that lipophilicity is the dominant factor determining the BBB permeability when the transporters systems are blocked either when using MDR1 ko mice, by saturation or by blocking the Pgp system. At 3 μM the transporters in the insect brain are active and they can be blocked by co-administration with verapamil, which increases the insect brain concentration for known Pgp substrates (Table 2). As it is seen from Table 2, four known CNS active compounds trazodone, citalopram, risperidone and desipramine are found to be Pgp substrates. However, it is obvious from the data obtained in the insect model that despite these compounds are Pgp substrates they are still

present in significant amounts in the insect brain. Thus, the ex vivo data suggests that these drugs are likely to have effect on the central nervous system.

The insect brain consists of glia cells. This together with the species difference implies that there may be differences between the functionality of the Pgp in rodents and insects. However, apart from trazodone the insect data are in accordance with the classification of the compounds obtained from Pgp-ko mice or when using the B-A/A-B ratio from MDCK-MDR1 (Mahar Doan et al., 2002; Doran et al., 2005; Feng et al., 2008). These data suggest that the insect ex vivo model can be used to identify Pgp substrates. However, further investigations of the sequence homology between the grasshopper and vertebrate Pgps are needed to get a deeper understanding of the Pgp similarities.

How to use the ex vivo model: The data obtained with the ex vivo insect model emphasizes the complexity of the transport mechanisms. As in vertebrates the grasshopper brain uptake shows that Pgp substrates can be CNS drugs (DeSalvo et al. 2011). On the other hand Pgp substrates can saturate the Pgp transporters and these may falsely be considered as potential CNS drugs. Substrates have different affinities to the different transporter systems and the concentration at which the transporters are saturated is compound dependent (Matsson et al., 2009). The data obtained here suggest that the insect ex vivo model may be useful to identify and test saturation of transport mechanisms.

The insect ex vivo brain uptake model has higher degree of correlation with in situ perfusion data than MDCK-MDR1. A main difference between the insect ex vivo and MDCK models is the cell layer, which in the insect brain barrier consists of glia cells while MDCK is based on epithelial cells. In the ex vivo model the biological events inside the brain are still active. These events include non-specific binding to brain lipids and proteins and the brain uptake results are influenced by non-specific binding to the brain tissue, i.e. higher brain tissue binding will push the equilibrium

over the BBB towards higher brain concentration. However, the insect brain uptake does not say anything about the free fraction in the brain. To get knowledge about the potential therapeutic effects of a compound, both the insect uptake as well as the brain free fraction should be determined.

In conclusion, the developed insect ex vivo BBB model allows classification of compounds as high, low or intermediate permeating compounds. At high exposure concentrations the transport efflux may be diminished and the ex vivo data correlates to in situ data obtained in rodents. Thus, at 10 μM the ex vivo model is useful for BBB permeability measurements. At 3 μM the Pgp efflux mechanism is pronounced and there is a lower correlation to in situ data. Pgp substrates can be identified by co-administration with a Pgp inhibitor like verapamil.

Acknowledgements

The authors are grateful to Kirsten Andersen, Chief Technician, and Marianne Reni Andersen, Technician, University of Copenhagen for assisting the LC-MS analysis and Laurent David, Principal Scientist, Lundbeck A/S for computational support.

Authorship Contribution

Participated in research design: O. Andersson, G. Andersson and Nielsen

Conducting experiment: O. Andersson and Hellman

Contributed new reagents or analytical tools: Hansen

Performed data analysis: G. Andersson and Nielsen

Wrote or contributed to the writing of the manuscript: Svenstrup, Badolo, Hansen, Andersson and Nielsen

References

Abbott JN, Begley DJ, Preston JE, Romero NIA. BLOOD-BRAIN BARRIER CONSORTUM, King's College London, November 9th, 2012: 6.1-6.5.

Abbott JN, Patabendige AAK, Dolman DEM, Yusof SR, Begley DJ (2010) Structure and function of the blood-brain barrier. *Neurobiol Dis* **37**: 13-25.

Abbott JN, Rönnbäck L, Hansson E (2006) Astrocyte-endothelial interactions at the blood-brain barrier. *Nat Rev Neurosci* **7**: 41-53.

Abbott NJ, Dolman DEM, Patabendige AK (2008) Assays to predict drug permeation across the blood-brain barrier, and distribution to brain. *Curr Drug Metab* **9**: 901-910.

Banerjee S, Bhat MA. (2006) Neuron-glia interactions in the blood-brain barrier formation. *Annu Rev Neurosci* **30**: 235-258.

Bundgaard M, Abbott JN (2008) All vertebrates started out with a glial blood-brain barrier 4-500 million years ago. *Glia* **56**: 699-708.

Cecchelli R, Berezowski V, Lundquist S, Culot M, Renftel M, Dehouck MP, Fenart L (2007) Modelling of blood-brain barrier in drug discovery and development. *Nat Rev Drug Discov* **6**: 650-661.

Danemann R, Barres BA (2005) The blood-brain barrier- Lessons from moody flies. *Cell* **123**: 9-12.

Dagenais C, Avdeef A, Tsinmann O, Dudley A, Beliveau R (2009) P-glycoprotein deficient mouse in sitblood–brain barrier permeability and its prediction using an in combo PAMPA model. *Eur J Pharm Sci* **38**; 121-137.

DeSalvo MK, Mayer N, Mayer F, Bainton RJ (2011) Physiologic and anatomic characterization of the brain surface glia barrier of *Drosophila*. *Glia* **59**: 1322-1340.

Di L, Kerns EH, Bezar IF, Petusky SL, Huang Y. (2009) Comparison of blood–brain barrier permeability assays: in situ brain perfusion, MDR1-MDCKII and PAMPA-BBB *J Pharm Sci* **98**; 1980-1991.

Doran A, Obach RS, Smith BJ, Hosea NA, Becker S, Calegari E. Chen C, Chen X, Choo E, Cianfrogna J, Cox L, Gibbs JP, Gibbs MA, Hatch H, Hop CECA, Kasman IN, LaPerle J, Liu J, Liu X, Logman, M, Maclin D, Nedza FM, Nelson F, Olson E, Rahematpura S, Raunig D, Rogers S, Schmidt K, Spracklin DK, Szwc M, Troutman M, Tseng E, Tu M, Van Deusen JW, Venkatakrishnan, Walens G, Wang EQ, Wong D, Yasgar AS, Zhang C (2005) The impact of P-glycoprotein on the disposition of drugs targeted for indications of the central nervous system: evaluation using the MDR1A/1B knockout mouse model. *Drug Metab Dispos* **33**: 165-174.

Feng B, Mills JB, Davidson RE, Mireles RJ, Janiszewski JS, Troutman MD (2008) *In vitro* P-glycoprotein assays to predict the *In vivo* interactions of P-glycoprotein with drugs in the central nervous system. *Drug Metab Dispos* **36**: 268-275.

Freeman MR, Doherty J (2006) Glial cell biology in *Drosophila* and vertebrates, *Trends Neurosci* **29**; 82-90.

Garberg P, Ball M, Borg N, Cecchelli R, Fenart L, Hurst RD, Lindmark T, Mabondzo A, Nilsson JE, Raub TJ, Stanimirovic D, Terasaki T, Öberg JO, Österberg T(2005) *In vitro* models for the blood-brain barrier. *Toxicol In Vitro* **19**: 299-334.

Geldenhuys WJ, Allen DD, Bloomquist JR (2012) Novel models for assessing blood-brain barrier drug permeation. *Expert Opin Drug Metab Toxicol* **6**: 647–653.

Liu X, Chen C, Smith BJ. (2008) Progress in brain penetration evaluation in drug discovery and development. *J Pharmacol Exp Ther* **325**: 349-356.

Mahar Doan KM, Humphreys JE, Webster LO, Wring SA, Shampine LJ, Serabjit-Singh CJ, Adkison KK, Polli JW (2002) Passive permeability and P-glycoprotein-mediated efflux differentiate central nervous system (CNS) and non-CNS marketed drugs. *J Pharmacol Exp Ther* **303**: 1029-1037.

Matsson P, Pedersen JM, Norrinder U, Bergström CAS, Artursson P (2009) Identification of novel specific and general inhibitors of the three major human ATP-binding cassette transporters P-gp, BCRP and MRP2 among registred drugs. *Pharm Res* **26**, 1816-1831.

Mayer F, Mayer N, Chinn L, Pinsonneault RL, Kroetz D, Bainton RJ (2009) Evolutionary conservation of vertebrate blood-brain barrier chemoprotective mechanisms in *Drosophila*. *J Neurosci* **29**: 3538-3550.

Mensch J, Oyarzabal J, Mackie C, Augustijns P. (2009) In vivo, in vitro and in silico methods for small molecule transfer across the BBB. *J Pharm Sci* **98**: 4429-4468.

Molecular Operating Environment (MOE), 2012.10; Chemical Computing Group Inc., 1010 Sherbooke St. West, Suite #910, Montreal, QC, Canada, H3A 2R7, 2012.

Murakami H, Takanaga H, Matsuo H, Ohtani H, Sawada Y (2000) Comparison of blood-brain barrier permeability in mice and in rats using in situ brain perfusion technique *Am J Physiol Heart Circ Physiol* **279**: 1022-1028.

Nielsen PA, Andersson O, Hansen SH, Simonsen KB, Andersson G (2011) Models for predicting blood-brain barrier permeation. *Drug Discov Today* **16**: 472-475.

Polli JW, Wring SA, Humphreys JE, Huang L, Morgan JB, Webster LO. Serabjit-Singh CS (2001) Rational use of in vitro P-glycoprotein assays in drug discovery. *J Pharmacol Exp Ther* **299**: 620-628.

Stork T, Engelen D, Krudewig A, Silies M, Bainton RJ, Klämbt C (2008) Organization and function of the blood-brain barrier in *Drosophila*. *J Neurosci* **28**: 587-597.

Weiss J, Dorman SMG, Martin-Facklam M, Kerpen CJ, Ketabi-Kiyanvash NK, Haefeli WE (2003) Inhibition of P-glycoprotein by newer antidepressant. *J Pharmacol Exp Ther* **305**: 197-204.

Wu VM, Beitel GJ. (2004) A junctional problem of apical proportions: Epithelial tube-size control by septet junctions in the Drosophila tracheal system. *Curr Opin Cell Biol* **16**: 493-499.

FOOTNOTE

This work was supported by The Danish National Advanced Technology Foundation [Grant 023-2011-3].

FIGURE LEGENDS

Figure 1. Diagram showing the ex vivo experiment process and the relation among the insect brain, hemolymph, and barrier cells.

Figure 2. Distribution of drug concentrations measured in the dessert locust brain after 15 minutes using exposure concentration of 10 μM (n=3 and two brains in each vial). Known CNS drugs are shown in dark gray while peripheral drugs are shown in light gray.

Figure 3. Distribution of drug concentrations measured in the dessert locust brain after 15 minutes using exposure concentration of 3 μM (n=3 and two brains in each vial). Known CNS drugs are shown in dark gray while peripheral drugs are shown in light gray.

Figure 4. Correlations between LogPS extracted from Dagenais et al., 2009 and the different permeability models used in this work: (**a**) apparent permeability measured using MDCK-MDR1 cells, (**b**) logarithm of grasshopper brain concentration obtained after using 10 μM exposure concentration, (**c**) logarithm of grasshopper brain concentration obtained after using 3 μM exposure concentration, (**d**) logarithm of grasshopper brain concentration obtained after 3 μM exposure concentration + verapamil. Only compounds known not to be Pgp substrates are included in chart 4**b.**

Figure 5. Correlation between the calculated lipophilicity (cLogP) using MOE (Molecular Operating system, 2012) and brain uptake obtained from in situ experiments (Dagenais et al., 2009) (**a**) or the logarithm of grasshopper brain concentration using 10 μM exposure concentration (**b**).

JPET Fast Forward. Published on May 13, 2013 as DOI: 10.1124/jpet.113.205476
This article has not been copyedited and formatted. The final version may differ from this version.

Table 1

Brain uptake measurements extracted from the literature or from dessert locust brain concentrations

Drug (CAS-No)	**Class**	**MW**	**cLogP**[a]	**Ctot 3µM (S.D.)**	**Ctot 3µM + verapamil (S.D.) in µM**	**Ctot 10µM (S.D.) in µM**	**Papp (10^{-6}) MDCK-MDR1**	**LogPS in situ**[d]
Digoxin (20830-75-5)	Neutral	781	1.4	0	0.2 (0.0)	0.8 (0.1)	0.1[b]	-4.5
Cimetidine (51481-61-9)	Neutral	252	0.2	0.2 (0.0)	0.2 (0.0)	0.4 (0.0)		-4.1
Cetirizine (83881-51-0)	Zwitterion	389	2.1	0.4 (0.1)	0.8 (0.2)	2.2 (0.4)		-3.7
Quinidine (56-54-2)	basic	324	2.8	0.7 (0.0)	1.9 (0.2)	3.2 (0.8)	1.2[b]	-2.1
Warfarin (81-81-2)	neutral	308	2.9	1.4 (0.1)	1.6 (0.1)	4.7 (1.2)	78[c]	-2.1
Citalopram (59729-33-8)	basic	324	3.1	0.7 (0.1)	1.1 (0.1)	4.6 (0.1)	11[b]	-2.0
Risperidone (106266-06-2)	basic	410	2.7	1.9 (0.2)	4.3 (0.3)	8.2 (0.5)	5.0[b]	-1.8
Loperamide (53179-11-6)	basic	477	4.7	0.6 (0.2)	2.3 (0.8)	6.2 (0.6)	2.6[b]	-1.7
Bupropion (34841-39-9)	basic	240	3.2	1.8 (0.4)	1.7 (0.2)	9.7 (2.2)	29[b]	-1.5
Trazodone (19794-93-5)	basic	372	3.9	1.1 (0.0)	4.9 (1.8)	9.2 (1.8)	17[b]	-1.5
Haloperidol (52-86-8)	basic	376	3.8	2.1 (0.3)	3.4 (1.0)	13.4(3.0)	28[c]	-1.5
Carbamazepine (298-46-4)	neutral	236	2.4	5.2 (0.3)	6.1 (0.4)	16.0 (0.9)	31[c]	-1.3
Propranolol (525-66-6)	basic	259	2.8	1.1 (0.2)	1.9 (0.4)	8.1 (0.8)	26[b]	-2.0
Fluoxetine (54910-89-3)	basic	309	4.6	4.1 (2.2)	9.2 (2.2)	19.8 (0.8)	8.1[b]	-1.2
Amitriptyline (50-48-6)	basic	277	4.9	2.1 (0.5)	4.2 (1.8)	15.0 (2.9)	3.6[c]	-0.7
Atenolol (29122-68-7)	basic	266	-0.1	0	0	0.2 (0.0)	0.1[c]	
Paroxetine (61869-08-7)	basic	329	4.2	6.5 (2.1)	8.2 (0.3)	25.0 (1.4)	5.5[b]	
Ranitidine (66357-35-5)	basic	314	0.7	0	0	0.2 (0.0)	0.3[b]	
Caffeine (58-08-2)	neutral	194	0.0	1.7 (0.1)	1.9 (0.2)	5.5 (0.1)	20[c]	

JPET Fast Forward. Published on May 13, 2013 as DOI: 10.1124/jpet.113.205476
This article has not been copyedited and formatted. The final version may differ from this version.

Desipramine (50-47-5)	basic	266	4.5	1.8 (0.4)	2.7 (0.2)	11.0 (2.8)	5.6[c]
Lincomycin (154-21-2)	basic	407	1.3	0	0	0.3 (0.1)	
Norfloxacin (70458-96-7)	zwitterion	319	-0.8	0.3 (0.0)	0.2 (0.0)	0.8 (0.3)	0.1[b]
Methotrexate (59-05-2)	acid	454	-0.5	0	0	0.2 (0.0)	
Dexamethasone (50-02-2)	neutral	392	1.8	0.2 (0.0)	0.3 (0.0)	1.0 (0.2)	2.6[b]
Cyclosporin A (59865-13-3)	neutral	1203	>4	0.4 (0.0)	0.4 (0.0)	2.6 (0.3)	

[a] cLogP calculated using MOE (Molecular Operating system, 2012)

[b] This work

[c] Di et al. 2009

[d] Dagenais et al., 2009

JPET Fast Forward. Published on May 13, 2013 as DOI: 10.1124/jpet.113.205476
This article has not been copyedited and formatted. The final version may differ from this version.

Table 2

Identification of Pgp substrates

Non Pgp substrates[a]	Ratio[b]	Pgp substrates[a]	Ratio[b]
Cimetidine	1.1	Cetirizine	2.1*
Warfarin	1.2*	Quinidine	2.8**
Bupropion	1.0	Risperidone	2.3**
Carbamazepine	1.2*	Loperamide	3.5*
Paroxetine	1.3	Trazodone	4.7*
Caffeine	1.1	Citalopram	1.5**
Norfloxacin	0.9	Propranolol	1.7*
CsA	1.0	Desipramine	1.5*
		Dexamethasone	1.6*
		Digoxin	>1.5

[a] Compounds where the ratio (Ctot 3 μM + Verapamil)/(Ctot 3 μM) is above 1.5 are defined as Pgp substrates

[b] (Ctot 3 μM + Verapamil)/(Ctot 3 μM); *P<0.05, **P<0.01

Figure 1

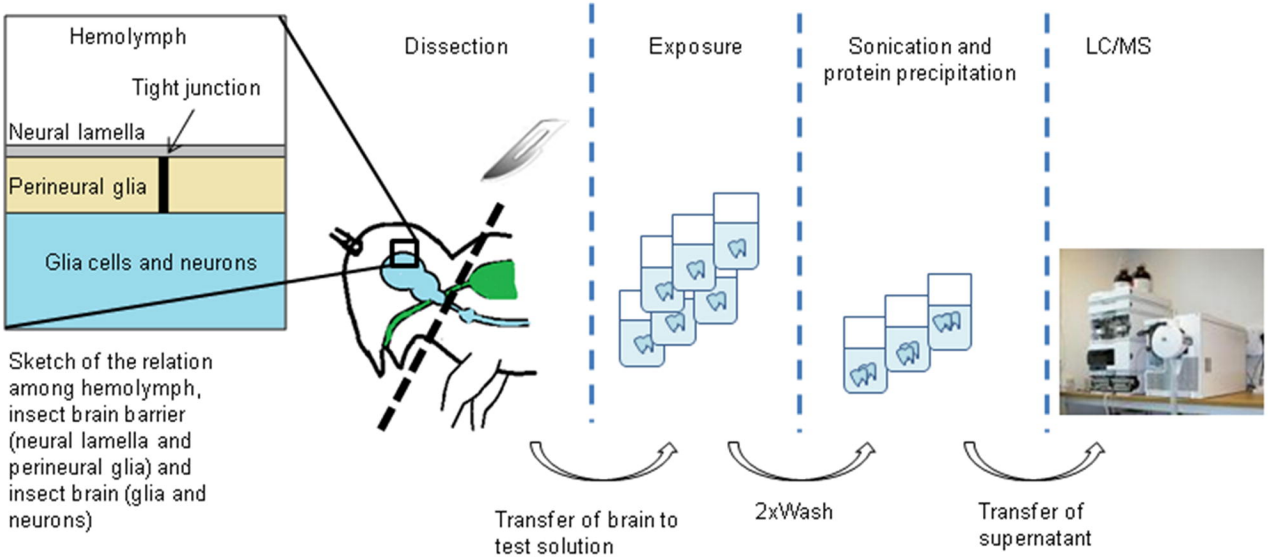
Hemolymph
Tight junction
Neural lamella
Perineural glia
Glia cells and neurons
Sketch of the relation among hemolymph, insect brain barrier (neural lamella and perineural glia) and insect brain (glia and neurons)
Dissection
Exposure
Sonication and protein precipitation
LC/MS
Transfer of brain to test solution
2xWash
Transfer of supernatant

Figure 2

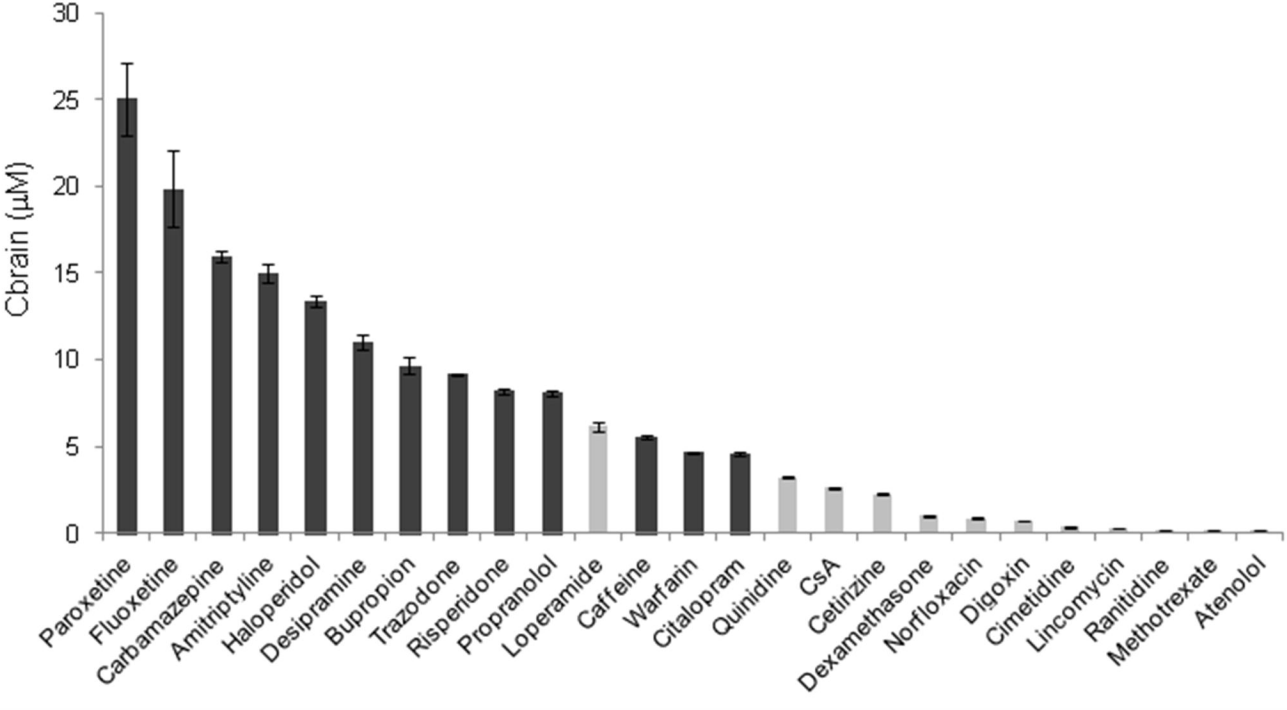
Cbrain (μM)
30
25
20
15
10
5
0
Paroxetine
Fluoxetine
Carbamazepine
Amitriptyline
Haloperidol
Desipramine
Bupropion
Trazodone
Risperidone
Propranolol
Loperamide
Caffeine
Warfarin
Citalopram
Quinidine
CsA
Cetirizine
Dexamethasone
Norfloxacin
Digoxin
Cimetidine
Lincomycin
Ranitidine
Methotrexate
Atenolol

Figure 3

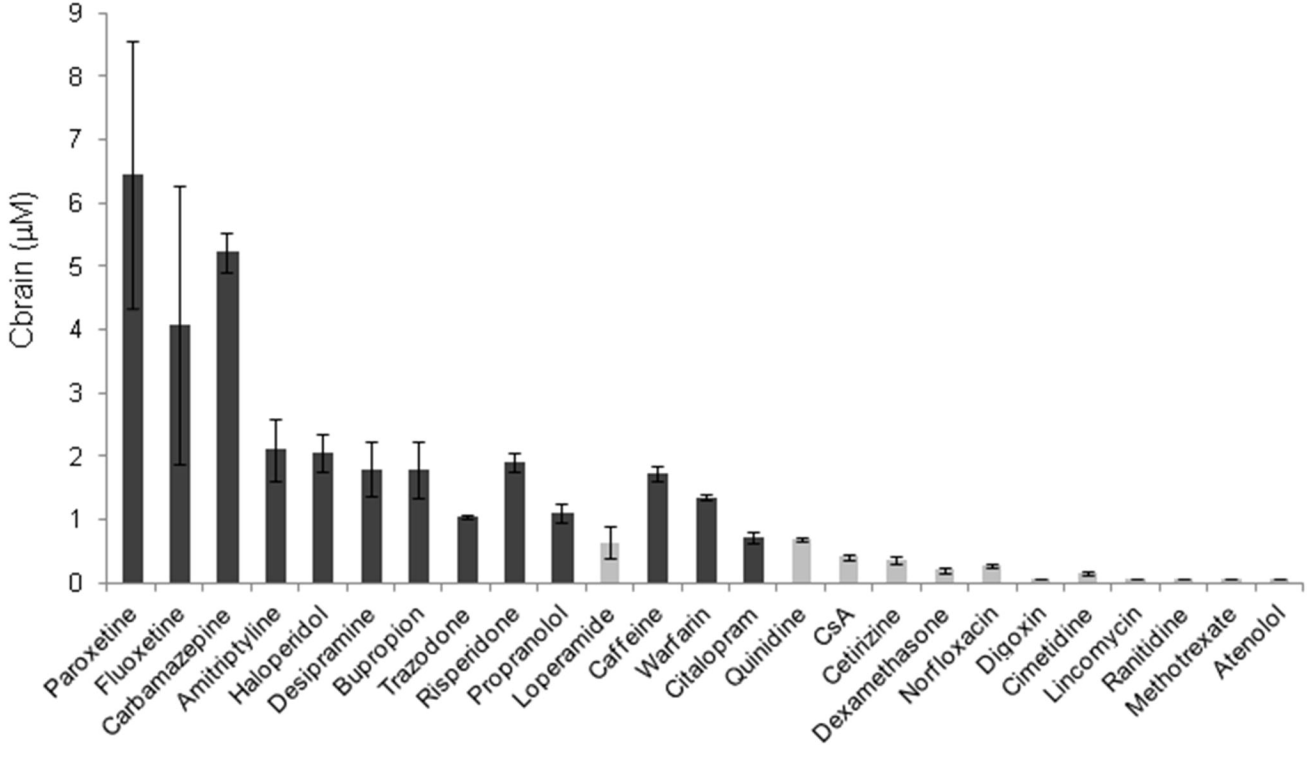
Cbrain (μM)
0
1
2
3
4
5
6
7
8
9
Paroxetine
Fluoxetine
Carbamazepine
Amitriptyline
Haloperidol
Desipramine
Bupropion
Trazodone
Risperidone
Propranolol
Loperamide
Caffeine
Warfarin
Citalopram
Quinidine
CsA
Cetirizine
Dexamethasone
Norfloxacin
Digoxin
Cimetidine
Lincomycin
Ranitidine
Methotrexate
Atenolol

Figure 4

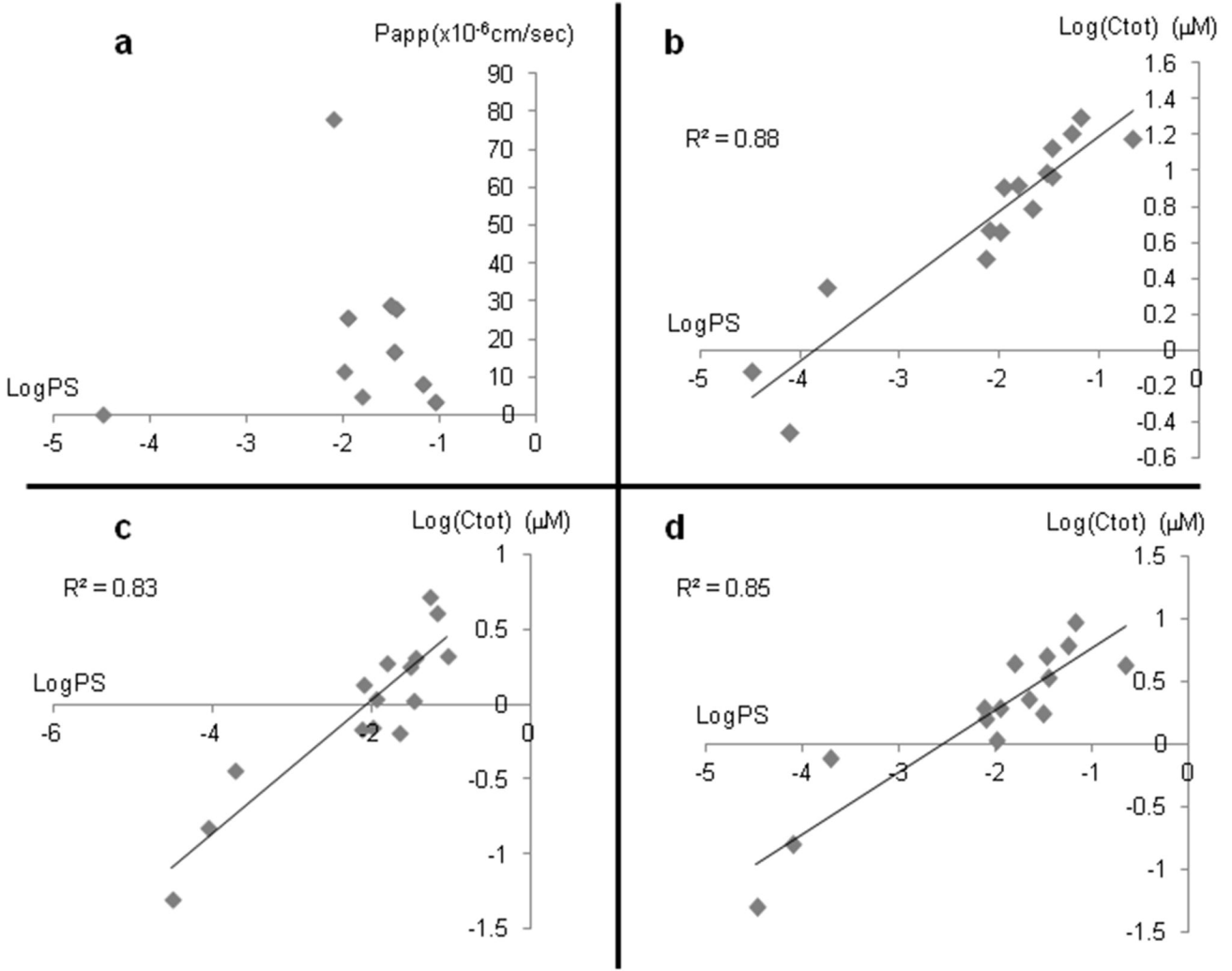
a
Papp(x10-6cm/sec)
LogPS
b
Log(Ctot) (µM)
R² = 0.88
LogPS
c
Log(Ctot) (µM)
R² = 0.83
LogPS
d
Log(Ctot) (µM)
R² = 0.85
LogPS

Figure 5

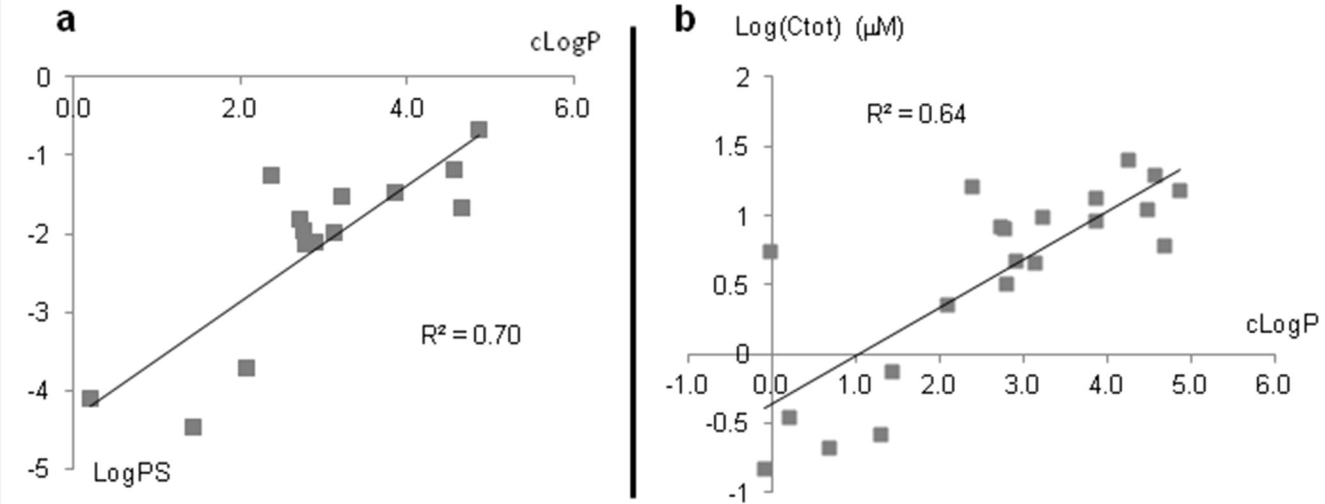
a
cLogP
0
0.0
2.0
4.0
6.0
-1
-2
-3
-4
-5
LogPS
R² = 0.70
b
Log(Ctot) (µM)
2
1.5
1
0.5
0
-0.5
-1
-1.0
0.0
1.0
2.0
3.0
4.0
5.0
6.0
cLogP
R² = 0.64